*Korean J. Chem. Eng.*, **31**(9), 1674-1680 (2014)
DOI: 10.1007/s11814-014-0117-0

pISSN: 0256-1115
eISSN: 1975-7220

# Effect of crosslinker feed content on catalaytic activity of silver nanoparticles fabricated in multiresponsive microgels

**Zahoor Hussain Farooqi*,†, Shanza Rauf Khan*, Tajamal Hussain*, Robina Begum**, Kiran Ejaz*, Shumaila Majeed*, Muhammad Ajmal***, Farah Kanwal*, and Mohammad Siddiq*****

*Institute of Chemistry, University of the Punjab, New Campus Lahore 54590, Pakistan
**Centre for Undergraduate Studies, University of the Punjab, New Campus Lahore 54590, Pakistan
***Department of Chemistry, Quaid-I-Azam University, Islamabad 45320, Pakistan
(*Received 21 September 2013 • accepted 17 April 2014*)

**Abstract**−We investigated the effect of crosslinking density of poly(N-isopropyl acrylamide-co-acrylic acid) microgels on catalytic activity of silver nanoparticles fabricated hybrid microgels. Multiresponsive poly(N-isopropyl acrylamide-co-acrylic acid) microgels with 2, 4, 6 and 8 mole percentage of N,N-methylene-bis-acrylamide were synthesized by emulsion polymerization. These microgels were characterized by dynamic light scattering and were used as microreactors to synthesize silver nanoparticles. Hybrid system was characterized by ultraviolet-visible spectroscopy. The catalytic activity of hybrid microgels with different crosslinker content was compared by studying the reduction of p-nitrophenol as a model reaction. Kinetics of reaction was monitored by spectrophotometry. The value of the apparent rate constant decreases from 0.568 to 0.313 $min^{-1}$, when content of crosslinker are increased from 2 to 8 mole percentage respectively. This decreases in value of apparent rate constant is due to increase in diffusional barrier offered by high crosslinking of polymer network at high mole percentages of N,N-methylene-bis-acrylamide.

Keywords: Microgels, Crosslinking Density, Hybrid Microgels, Catalytic Activity

## INTRODUCTION

Nanoparticles have attracted great attention for sensors [1-4], photonics [5-8], surface enhanced Raman spectroscopy [9-11], medicine [12,13], printable electronics [14,15], antimicrobial paints [16-18], and catalysis [19-21] due to their high surface area to volume ratio and extremely different properties from bulk materials [22,23]. Different nanoparticles like silver (Ag) [24,25], copper (Cu) [26,27], gold (Au) [28], palladium (Pd) [29,30], platinum (Pt) [31] and cobalt (Co) [32], have been employed for efficient catalysis of organic compounds like p-nitrophenol (p-NP) [33], o-nitrophenol [34], m-nitrophenol [35], nitrobenzene [36], butyraldehyde [37] and methylene blue [38], inorganic complexes like hexacyanoferrate (III) [39], and gases like carbonmonoxide [40]. Aggregation of naked nanoparticles is the main problem in catalysis [20]. The surface area of nanoparticles decreases as a result of aggregation, which results in reduction in rate of catalysis. Immobilization or encapsulation of nanoparticles on/within some supporting material is the classical method to solve this problem. Polymeric matrices like microgels [41,42], polyelectrolyte brushes [43] and dendrimers [44], or inorganic oxides like silica [45], alumina [46] and titania [47], have achieved great success as supporting material to resist aggregation of metal nanoparticles in the field of catalysis. Among all these classes, microgels are being largely employed as a stabilizer for nanoparticles due to comprehensive control of structure and visco-elasticity of microgels on stabilization of nanoparticles, because incorporated charged comonomers in microgels network keep nanoparticles intact while crosslinking resist aggregation by imposing physical barrier [48]. Moreover, the multiresponsiveness of microgels helps to tune catalytic activity of nanoparticles. Temperature-sensitive monomers like N-isopropyl acrylamide (NIPAM) are often copolymerized with pH sensitive comonomers (like acrylic acid (AAc), maleic acid, methacrylic acid etc., to synthesize multiresponsive microgel spheres [49,50]. These minute spheres can manipulate catalytic activity of nanoparticles by switching the size of microgels according to pH and temperature of medium [51,52]. These parameters have been used in the reported literature to tune the catalytic activity of nanoparticles. Liu et al. tuned the catalytic activity of Ag-P(NIPAM) hybrid microgels in response to temperature for catalytic degradation of 4-NP [53]. They also prepared Ag-P(S)/P(NIPAM) hybrid core-shell particles and studied the effect of temperature on the value of $k_{app}$ for catalysis of p-NP [54]. They did not study the influence of crosslinking on the value of $k_{app}$. Other catalysis parameters like catalyst dosage, concentration of reducing/oxidizing agent and concentration of substrate have also been studied by different scientists [21,55]. Sahiner et al. studied the effect of concentration of catalyst and sodium borohybride ($NaBH_4$) on catalysis of p-NP and o-nitrophenol by cobalt-poly(2-acrylamido-2-methyl-1-propansulfonic acid) hybrid microgels [34]. However, the mole percentage of crosslinker in microgels can be a new parameter to tune the catalytic activity of nanoparticles. According to best of our knowledge no one has reported it yet for microgels. Susana et al. used nanocomposites which have Au nanoparticles encapsulated in P(NIPAM) network. P(NIPAM) network has different mole ratio of BIS [56]. They studied these microgels for degradation of $[Fe(CN)_6]^{-3}$. The novelty of the present work lies in use of this parameter for microgels for cata-

†To whom correspondence should be addressed.
E-mail: zhfarooqi@gmail.com

lytic degradation of p-NP. Nanoparticles are not only at the center here, but they are fabricated in the whole network of these microgels. The crosslinker not only provides strength to microgels and fabricates network of microgels, but also controls the sieve size of its network [57]. The effect of mole percentage of crosslinker on structure of pure microgels has been studied previously. Varga et al. studied the effect of cosslinker on swelling ratio and internal structure of poly(N-isopropylacrylamide) [P(NIPAM)] microgels [58]. It has been reported that a high concentration of crosslinker creates an extensive and dense network of microgels; thus mesh size is reduced [57]. But still no one has tried to use it as parameter to control catalytic activity of nanoparticles. We thought that increase in crosslinking density can decrease rate by posing diffusional barrier to reactant molecules.

We studied the effect of crosslinking density by increasing crosslinker content on size of silver nanoparticles and rate of reduction of p-NP in aqueous medium. We explain that that the extent of crosslinking of spherical microspheres can modulate surface plasmon resonance wavelength ($\lambda_{SPR}$) of nanoparticles and their catalytic activity up to a large extent.

## EXPERIMENTAL WORK

### 1. Materials

N-isopropylacrylamide (NIPAM), acrylic acid (AAc), sodium dodecylsulfate (SDS), *N,N*-methylenebis(acrylamide) (BIS) and p-Nitrophenol (p-NP) were purchased from Sigma-Aldrich, while sodium borohydride ($NaBH_4$) was obtained from Scharlau Company. All chemicals were used as such except AAc which was purified by filtration through alumina ($Al_2O_3$) under reduced pressure. Distilled water was used for all solutions preparations, dialysis, synthesis and catalytic reduction.

### 2. Synthesis of Differently Crosslinked P(NIPAM-co-AAc) Microgels

NIPAM, AAc, BIS, SDS and 95 mL water were added into a three-necked flask. Then this reaction mixture was continuously stirred at 70 °C under nitrogen gas ($N_2$) purge. After 30 min, 5 mL of freshly prepared 0.05 M APS was added dropwise into it. Reaction was further continued for 5 hr after appearance of turbidity. Then prepared microgels were cooled and dialyzed for 1 week through Spectra/Por® molecular porous membrane tubing (Fisher Scientific) having MWCO 12000-14000 against a daily exchange of distilled water at room temperature (~22 °C). All microgels were prepared by same method and details of their compositions are given in Table 1.

### 3. Synthesis of Hybrid Microgels

25 mL of earlier prepared microgels and 19.9 mL distilled water were added into a three-necked round bottom flask, and the reaction mixture was stirred under continuous $N_2$ purge for half an hour. Then 0.15 mL of 0.1 M silver nitrate ($AgNO_3$) solution were added into it at room temperature. After 30 min, freshly prepared solution of $NaBH_4$ (0.01 g in 5 mL) was added and reaction was proceeded for 90 min. Prepared Ag-P(NIPAM-co-AAc) hybrid microgels were purified through dialysis of 1 hour against distilled water using Spectra/Por® membrane. All hybrid microgels Ag-(PBIS-A), Ag-(PBIS-B), Ag-(PBIS-C) and Ag-(PBIS-D) were prepared, respectively, from PBIS-A, PBIS-B, PBIS-C and PBIS-D by following the same method.

**Table 1. Feed composition of P(NIPAM-co-AAc) microgels**

| Microgel samples | Mole percentage | | | BIS/NIPAM mole ratio | SDS/G |
|---|---|---|---|---|---|
| | NIPAM | AAc | BIS | | |
| PBIS-A | 93 | 5 | 2 | 0.0215 | 0.05 |
| PBIS-B | 91 | 5 | 4 | 0.0439 | 0.05 |
| PBIS-C | 89 | 5 | 6 | 0.0674 | 0.05 |
| PBIS-D | 87 | 5 | 8 | 0.0919 | 0.05 |

### 4. Catalytic Reduction of p-Nitrophenol

1.8 mL of 0.1 mM p-NP (pH=8) and 0.5 mL of 20 mM $NaBH_4$ were added into cuvette and then 0.2 mL of 66% diluted Ag-(PBIS-A) was added into the reaction mixture. Spectra (range of 250-500 nm) were scanned after every minute using a UVD-3500 (Labomed, Inc.) spectrophotometer until absorbance decreased to a constant value at 400 nm. The same model catalytic reaction was carried out using the same method and quantitities in the presence of Ag-(PBIS-A), Ag-(PBIS-B), Ag-(PBIS-C) and Ag-(PBIS-D).

### 5. Characterization

FTIR spectra were obtained by Perkin Elmer, RX I FTIR spectrometer in near infrared range of 4,000-650 $cm^{-1}$. BI-200SM Laser light spectrometer of Brookhaven Instruments Corporation equipped with a BI-9000 AT digital time correlator and Helim-Neon (He-Ne) laser source (35 mW and 632.8 nm) was used for dynamic laser light scattering measurements of microgels.

## RESULTS AND DISCUSSIONS

### 1. Synthesis of P(NIPAM-co-AAc) Microgels with Different Crosslinking Densities

P(NIPAM-co-AAc) microgels were prepared by emulsion polymerization using methods reported previously [59]. This is an efficient method for synthesis of microgels, because it reduces chances of macrogelation. This polymerization gives high yield of monodisperse microspheres, because those polymer chains which have high molecular weight get inter-crosslinked rapidly [60]. In this way spherical particles of similar sizes are formed. Thus here we synthesized four compositions of microgels possessing different mole percentages of crosslinker by using this method.

Crosslinking and branching of polymer chains are two reactions which are taking place side-by-side during polymerization. BIS has greater reactivity with sulfate radicals as compared to AAc and NIPAM [61]. So incorporation of BIS within woven network of polymer is greater as compared to monomers at start of polymerization and a crosslinked network is fabricated. Concentration of BIS decreases with the progress of polymerization, so crosslinking within the network of microgels starts decreasing and branching of polymer chains increases. This difference of BIS concentration at different time produces microspheres which have greater crosslinking at core and more branching in network at periphery. When the percentage of BIS increases, the volume of core of microgel particles increases, because high BIS content develops crosslinks with greater number of polymer chains [59]. Thus, with decrease in NIPAM/BIS mole ratio, incorporation of monomers within particles increases, which in turn increases the percentage yield of microgel particles. High BIS content not only forms crosslinks with greater number of polymer chains

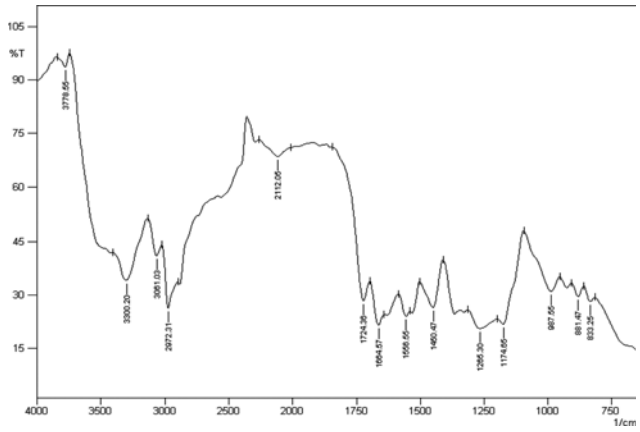


**Fig. 1. FTIR spectra of sample PBIS-D of p(NIPAM-co-AAc) microgel.**

but also develops greater number of crosslinks. Thus, the distance between two crosslinking points decreases and a dense network is fabricated at the core along with less uniform segment density distribution. On contrary, this leaves a very small amount of monomers at end of reaction for branching of polymer chains at periphery. Thus PBIS-D possesses greater volume of compact crosslinked core than PBIS-A and PBIS-A has greater volume of branched shell as compared to PBIS-D [58,62]. Varga et al. explained smaller and non-uniform distribution of segment density in highly crosslinked PNIPAM microgels and also provided a comparison of structure of a range of microgels which possess different NIPAM/BIS ratio [58].

**2. FTIR Analysis of P(NIPAM-co-AAc) Microgel**

Fig. 1 shows the FTIR spectrum of P(NIPAM-co-AAc) microgel (PBIS-D) in which a number of characteristic bands of different functional groups are present. FTIR spectrum is used here to confirm synthesis of P(NIPAM-co-AAc) microgels and incorporation of all functional groups into polymer network of microgels. The characteristic band of C=C around 1,600 $cm^{-1}$ is absent in Fig. 1, which indicates that polymerization has occurred at C=C reactive site and no unreacted monomers (NIPAM and AAc) are present in the prepared sample. Distinctive bands at 1,724.36 and 1,664.57 $cm^{-1}$ confirm the presence of C=O group of NIPAM and AAc, respectively [63]. Moreover, characteristic bands at 1,556.55 (N-H bending) and 1,450.47 (-$CH_2$- bending) $cm^{-1}$ also provide evidence of the presence of NIPAM and AAc in a woven network of microgels [49]. The band at 1,265.30 $cm^{-1}$ signifies the presence of -C-O group. Presence of -O-H group of -COOH, and N-H (stretching) of NIPAM and BIS is confirmed by respective bands at 2,972.31 and 3,300.20 $cm^{-1}$ [21]. Both these bands also signify the presence of frozen water within the microgel sample. In this way, bands of different functional groups in Fig. 1 indicate that polymerization has occurred, and NIPAM, AAc and BIS have been incorporated into the microgel structure.

**3. DLS Study of P(NIPAM-co-AAc) Microgels**

The values of hydrodynamic diameter of different samples of P(NIPAM-co-AAc) microgels at pH 3.7 and 11.2 are given in Table 2. Data of this table provides an evidence that P(NIPAM-co-AAc) microgels are pH responsive and the swelling ratio given in the Table 2 shows that the elasticity of microgels decreases with increase in mole percentage of BIS.

**Table 2. The hydrodynamic diameters of PBIS-A, PBIS-B, PBIS-C and PBIS-D microgels at pH 3.7 and 11.2 and at temperature 25 °C**

| Sample | Hydrodynamic diameter/nm | | Swelling ratio= $(d_{swollen}/d_{shrunken})^3$ |
|---|---|---|---|
| | pH=3.7 ($d_{shrunken}$) | pH=11.2 ($d_{swollen}$) | |
| PBIS-A | 168 | 338.8 | 30.52 |
| PBIS-B | 135 | 390 | 24.11 |
| PBIS-C | 143.5 | 362.3 | 16.09 |
| PBIS-D | 149.3 | 333 | 11.63 |

The value of $d_h$ at pH 3.7 is smaller as compared to that of pH 11.2 for all samples because AAc is in protonated form in acidic medium, but as pH is increased above $pk_a$ value of AAc (~4.5), carboxyl groups are converted into carboxylate ions [64]. Carboxylate ions are negatively charged, so $d_h$ increases as a result of electrostatic repulsion. Values mentioned in Table 2 also give evidence that the value of $(d_{swollen}/d_{shrunken})^3$ of PBIS-D is smaller than that of PBIS-A, PBIS-B and PBIS-C. It means that microgels having high crosslinking density are comparatively more rigid and less elastic [65]. Senff et al. studied temperature sensitivity of P(NIPAM) microgels having different crosslinking density [59]. They observed that elasticity of microgels decreases with increase in mole percentage of BIS. Our results are in agreement with this study. The variation in swelling ratio and elasticity of microgels by varying BIS content provides the basis for modulation of catalytic activity.

**4. Effect of Mole Percentage of BIS on Size Distribution**

Fig. 2 shows size distribution of microgels having 2, 4 and 8% crosslinker content at pH 5. Fig. 2 indicates that the size distribution as well as size of microgels decreases by increasing crosslinker content. Microgels are in swollen state at pH 5 [66]. With increase in mole percent of crosslinker, the size of microgels decreases because the crosslinker decreases the swelling ratio and increases rigidity. The effect of crosslinker content on size and size distribution of in-vivo synthesized silver nanoparticles within microgels has been already reported by Dong et al. [50]. They confirmed by TEM images that the size distribution of Ag nanoparticles becomes narrower when the content of the crosslinker increases. The UV-visible spectra of hybrid microgels shown in Fig. 3 support this fact. Thus our results are in exact agreement with previously reported results in literature.

**5. Effect of Mole Percentage of BIS on Size of In-vivo Synthesized Silver Nanoparticles**

Fig. 3 describes the effect of structure of microgels on shape, size and size distribution of nanoparticles within hybrid microgels at pH

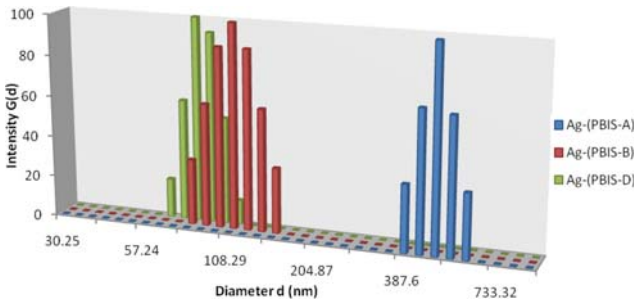


**Fig. 2. The size distribution of different samples of p(NIPAM-co-AAc) microgels at pH 5.**

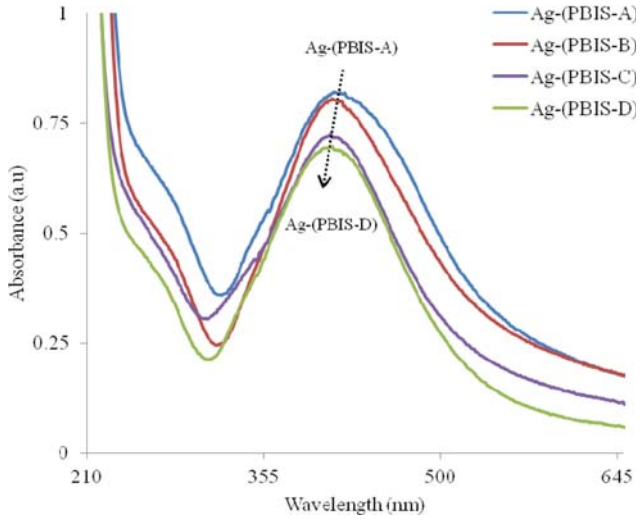


**Fig. 3. UV-VIS spectra of all hybrid microgels samples in aqueous medium at pH 9.88 and temperature 28±1 °C.**

9.88 (this pH was used for comparative analysis of $\lambda_{SPR}$ because this is the pH of the reaction mixture in which hybrid microgels later were used as catalyst). The single peak in ultravoilet-visible (UV-VIS) spectra of all hybrid samples shows that all samples are loaded with spherical nanoparticles [67]. $\lambda_{SPR}$ of all synthesized hybrid systems (PBIS-A, PBIS-B, PBIS-C and PBIS-D) are different in height and position in spectra because the structure of microgels acts as a template for tuning of characteristics of in-situ synthesized nanoparticles. The broad peak changes into a sharp peak with increase in BIS mole percentage along with blue shift in position of $\lambda_{SPR}$ in swollen state (Fig. 3). The blue shift in $\lambda_{SPR}$ with increase in BIS mole percentage indicates that the size of nanoparticles decreases, because sieve size of highly crosslinked microgels is comparatively smaller than less crosslinked samples [68,69]. Moreover, larger sieve sizes and radius of high mole percentage of BIS containing microgels provide larger free space for nanoparticles to become aggregate and grow, while high crsslinking offers a physical barrier against this aggregation. Thus, higher BIS-crosslinked microgels networks provide more stability to nanoparticles and help to synthesize nanoparticles of smaller size [70]. The concentration of precursor silver ions ($Ag^+$) and electrostatic attraction of ionic monomer (AAc) are constant for all microgels samples, so fixing of smaller number of $Ag^+$ by electrostatic attraction of AAc would be due to smaller sieves of PBIS-A than that PBIS-D. Thus, nanoparticle size becomes smaller and $\lambda_{SPR}$ decreases from 414 to 410 nm (Table 3) [58]. Heath et al. have also shown that bathochromic shift in $\lambda_{SPR}$ occurs by increase in size of Ag nanoparticles [71]. Broader size distribution of nanoparticles gives a wide band of $\lambda_{SPR}$, while a narrow size distribution gives a sharp band of $\lambda_{SPR}$. Less crosslinked microspheres have larger volume of non-uniform polymer segment density distribution, so sieve sizes are less homogeneous. So the majority of nanoparticles are not of nearly similar sizes that is why PBIS-A has a broader peak. Compact and highly dense microgels have large volume of core, so homogeneity of segment density distribution increases and narrow distribution of sizes among nanoparticles results [58]. This distribution is due to less difference between structure of core and periphery microgels; crosslinking density decreases from center to

**Table 3. Values of $\lambda_{SPR}$ and absorbance at $\lambda_{SPR}$ for all hybrid microgels samples at pH 9.88 and temperature 28±1 °C**

| Hybrid microgel samples | Surface plasmon resonance wavelength ($\lambda_{SPR}$)/nm | Absorbance (a.u) |
|---|---|---|
| Ag-(PBIS-A) | 414 | 0.821 |
| Ag-(PBIS-B) | 412 | 0.806 |
| Ag-(PBIS-C) | 411 | 0.724 |
| Ag-(PBIS-D) | 410 | 0.697 |

periphery in microgel particles. With decrease in BIS mole percentage, the non-uniformity within core increases and the size of core decreases; thus the peak gets broader as we move from sample having 8% BIS to 2% BIS. Moreover, Fig. 2 and values of absornace at $\lambda_{SPR}$ of all hybrid microgels in Table 3 show that absorbance of peak decreases as mole percentage of BIS increases. This decrease in absorbance is due to presence of highly crosslinked organic polymer network in vicinity of nanoparticles.

### 6. Catalytic Reduction of p-Nitrophenol

Catalytic reduction of p-NP is a model reaction that can be used to study the catalytic activity of hybrid microgels. All samples of microgels were used as catalyst for conversion of p-NP into p-amino phenol (p-AP). UV-VIS spectrophotometry was used to monitor the progress of reaction.

Fig. 4 gives the spectra of catalytic reduction of p-NP. p-NP and p-AP, both have $\lambda_{max}$ in UV-VIS range at 400 and 300 nm, respectively [28]. The peak at 400 nm decreases along with a concomitant increase in the peak at 300 nm during progress of the reaction after induction time. The spectrum has only two absorption peaks, which confirms that there are only two principal species present in the reaction mixture. $NaBH_4$ is not UV-VIS sensitive and its concentration is 100 times greater than that of p-NP in reaction mixture; thus the reaction follows pseudo-first-order kinetics [55].

$N_2$ was purged through all solutions to remove dissolved oxy-

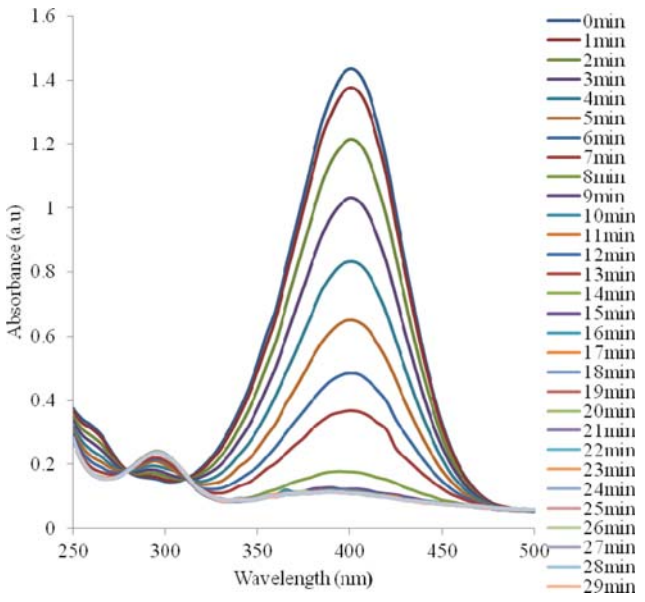


**Fig. 4. UV-VIS spectra of catalytic reduction of p-NP in aqueous medium in the presence of Ag-(PBIS-A) catalyst at pH 9.88 and temperature 28±1 °C.**

gen because $NaBH_4$ reacts faster with dissolved oxygen in water than with p-NP [43]. Resultantly, the time delay can be seen. Purging of $N_2$ reduces this possibility. But still Fig. 5 shows an induction time whose duration decreases with increase in mole percentage of BIS. This is due to slow activation of surface of metal catalyst due to slower diffusion rate of p-NP and $NaBH_4$ into microgels network [72]. Thus the value induction time for Ag-(PBIS-D) hybrid microgels is greater than for Ag-(PBIS-A) hybrid microgels.

Linear regions of plots of $\ln(A_t/A_o)$ versus time are shown in Fig. 6. The slope of the linear region of these plots was used for determination of $k_{app}$. The value of $\ln(A_t/A_o)$ linearly decreases with time. This shows that the reaction is first order with respect to concentration of p-NP as rate of reaction decreases linearly with decrease in concentration of p-NP. The slopes of all plots of Fig. 6 are different from each other. Therefore, rate constants for reduction catalyzed by Ag-(PBIS-A), Ag-(PBIS-B), Ag-(PBIS-C) and Ag-(PBIS-D) hybrid microgels were found to be 0.568, 0.359, 0.320 and 0.313 $min^{-1}$, respectively at 28±1 °C. This catalyst is more efficient than many previously reported catalysts as Ghosh et al. found values of $k_{app}$ equal to $75\times10^{-3}$ and $8.88\times10^{-3}$ $min^{-1}$ for 40 μL (0.1 mg/mL) suspension of Pt and Raney nickel (Ni) nanoparticles to reduce 20 μL of 4-NP (0.01 M) at 30±1 °C, respectively. They also used bi-metallic Ni-Pt (64 : 36) nano alloy and found $k_{app}$ equal to 0.0288 $min^{-1}$ [73]. Thus, our prepared catalyst is also more efficient than metallic nanoparticles and bi-metallic nanoalloys.

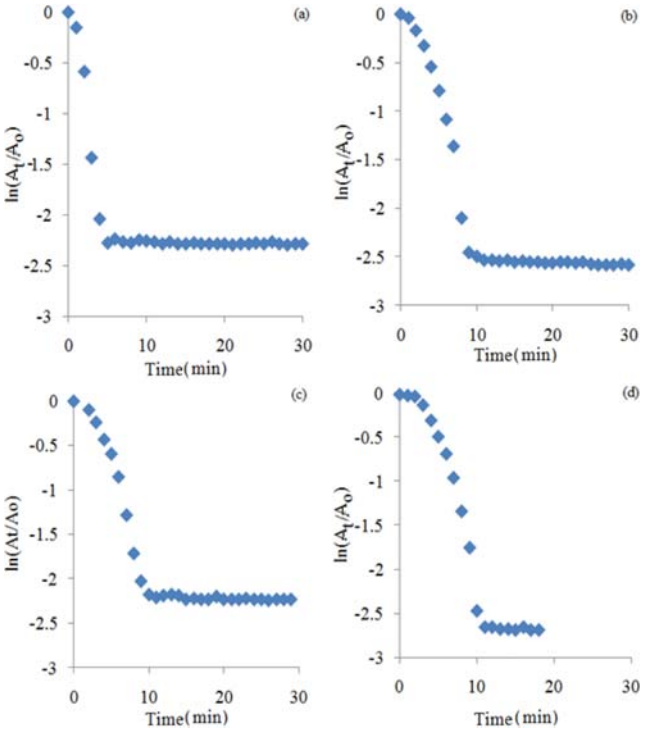


**Fig. 5. Plots of $\ln(A_t/A_o)$ as a function of time for reduction of p-NP in the presence of (a) Ag-(PBIS-A), (b) Ag-(PBIS-B), (c) Ag-(PBIS-C) and (d) Ag-(PBIS-D) hybrid microgels.**

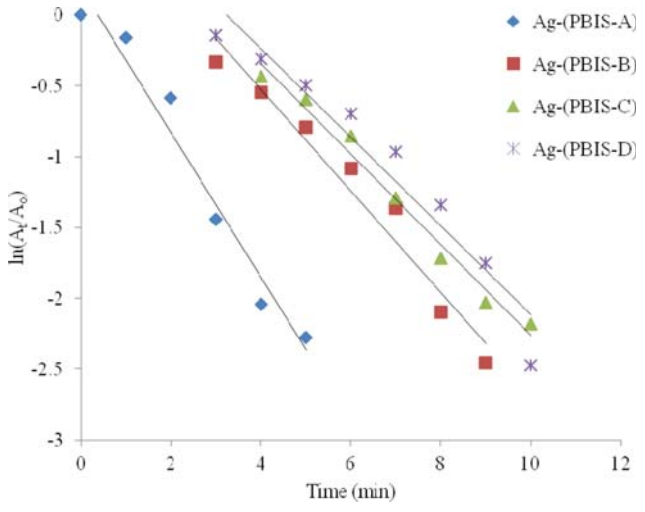


**Fig. 6. Plot of $\ln(A_t/A_o)$ versus time for catalytic reduction of p-NP by different hybrid microgels at pH 9.88 and temperature 28±1 °C in aqueous medium.**

## 7. Dependence of Apparent Rate Constant on Mole Percentage of BIS of Microgels

The dependence of $k_{app}$ on mole percentage of BIS is shown in Fig. 7. The values of $k_{app}$ are 0.568, 0.359, 0.320 and 0.313 $min^{-1}$ for 2, 4, 6 and 8 mole percentages of BIS, respectively. Thus the value of $k_{app}$ decreases with increase in content of BIS of microgels, which shows that diffusion of reactants, elasticity and sieve size of microgels decrease with increase in mole percentage of crosslinker. Earlier explained results of DLS confirm that the rigidity of microgels increases with BIS content. High amount of BIS increases crosslinking density, and a dense polymer network can more hinder movement of reactants towards the catalyst surface, so the reaction rate decreases. Moreover, swelling ratio and sieve size of microgel particles also become smaller due to high crosslinking. High crosslinking also increases rigidity and decreases elasticity of microgels, so the hydrodynamic radius of microgel particles in swelling state is smaller for higher percentage of BIS. Burmistrova et al. studied the variation in hydrodynamic radius of p(NIPAM-co-AAc) microgels containing 2, 5 and 10 mole percentage BIS using DLS [65]. They noticed that the swelling ratio of microgels decreases with

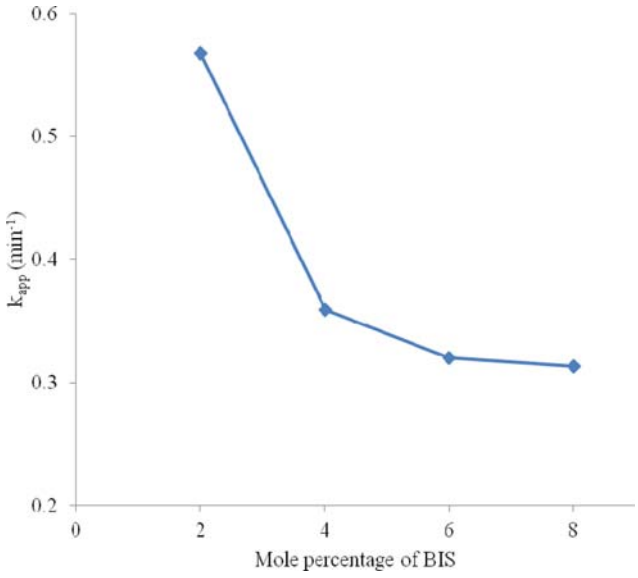


**Fig. 7. Dependence of $k_{app}$ on mole percentage of BIS of microgels.**

increase in content of crosslinker. Thus, it is inferred that high BIS content reduces space for diffusion of reactants towards the catalyst surface, as a result of which the value of apparent rate constant decreases with increase in crosslinker contents.

Fig. 7 shows that decrease in value of $k_{app}$ with increase in mole percentage of BIS is not linear. $k_{app}$ has larger extent of dependence on mole percentage of BIS, when mole percentage of BIS is between 2 and 4. But extent of this dependence is smaller as mole percentage of BIS increases from 4 to 8% within polymer of microgels [58]. This would be due to high crosslinking density of microgels having 4 mole percentage of BIS whose size is smaller, the structure is more rigid and possesses less elasticity than 2 mole percentage containing microgels (PBIS-A). And there are small variations among structure, size and elasticity of 4, 6 and 8 mole percentage containing microgels. Previously reported literature agrees that rigidity, size and crosslinking of microgels increase with mole percentage of BIS. It also confirms that structure and visco-elastic properties of microgels more rapidly vary, if mole percentage of BIS has smaller values, but the extent of this effect of BIS decreases when high mole percentages of BIS are employed [65,74]. Thus, here, values of $k_{app}$ for 2, 4, 6 and 8 mole percentage of BIS are not following a linear pattern.

**8. Dependence of Apparent Rate Constant on Catalyst Dosage**

Fig. 8 shows the dependence of $k_{app}$ of reduction of p-NP on dosage of Ag-(PBIS-A). 0.46, 0.51, 0.568 and 0.61 $min^{-1}$ values of $k_{app}$ were obtained, when 0.2 mL of 24%, 30%, 34% and 40% of Ag-(PBIS-A) hybrid microgel were employed for catalytic reduction of p-NP. Fig. 8 shows that the value of $k_{app}$ increases by increasing the concentration of hybrid microgels linearly. By increasing the amounts of catalyst, surface for catalysis increases [19]. Similar linear trend was observed by Zhang et al., when they used different catalyst dosages for reduction of p-NP [75]. Antonels et al. used ruthenium (Ru) incorporated dendrimers for reduction of p-NP [76]. They also observed that value of $k_{app}$ linearly increases by increasing concentration of hybrid dendrimers.

The plot of Fig. 8 does not pass through (0,0) co-ordinates. This plot has 0.298 $min^{-1}$ value of $k_{app}$ when no catalyst is used, so this reduction reaction is not kinetically hindered in the absence of nanoparticles. This non-zero and small value of $k_{app}$ indicates that reduction of p-NP with $NaBH_4$ occurs in the absence of catalyst, but with very low rate. So it would be impossible to monitor this reduction with UV-Visible spectrophotometry. Vadakkekara et al. also observed a very small value of $k_{app}$ of reduction of p-NP and 2-nitroaniline, when no hollow Ag nanospheres were employed [77]. Similar results were reported by Sahiner et al. [55] who observed that plot of dependence of $k_{app}$ of reduction of p-NP with $NaBH_4$ on amount of nickel-poly[2-acrylamido-2-methyl-1-propansulfonic acid] [Ni-p(AMPS)] catalyst did not pass through origin. The value of $k_{app}$ was found to be very small at zero catalyst dosage.

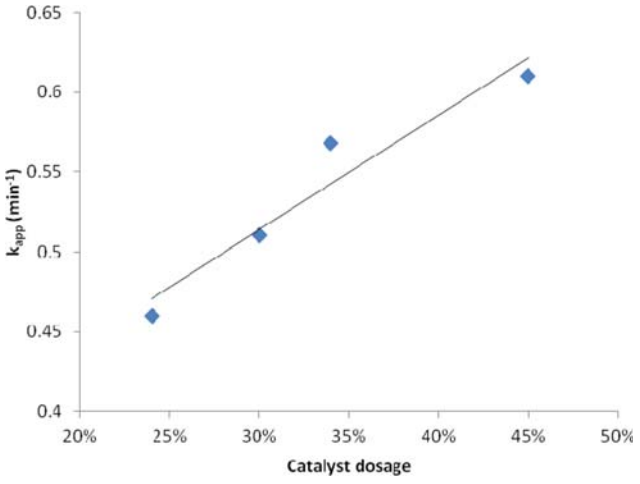


**Fig. 8. Dependence of $k_{app}$ of reduction of p-NP on catalyst dosage.**

## CONCLUSIONS

We have demonstrated that the internal structure of polymer matrix is significantly affected by variation in feed content of crosslinker. Increase of mole percentage of BIS in feed composition decreases sieve size of mesh and increases the volume of compact core in microgels; thus the size of in-vivo synthesized silver nanoparticles decreases. Low mole percentage of BIS also leads to high non-uniformity in density of polymer segments distribution, which increases size distribution of in situ synthesized nanoparticles. Moreover, crosslinking density also affects catalytic activity of hybrid microgels. A dense network of polymer matrix not only decreases the size of nanogates for diffusion of reactants, but also offers physical hindrance to movement of reactant species. That is why the value of apparent rate constant of catalytic reduction of p-nitrophenol decreases by increasing mole percentage of BIS. In this way, we can control the size and size distribution of nanoparticles and their catalytic activity by varying crosslinker contents of microreactor microgels.

## ACKNOWLEDGEMENT

This work was supported by University of the Punjab Lahore, Pakistan under university grant for the Fiscal Year 2012-2013.

## REFERENCES

1. A. Y. Nazzal, L. Qu, X. Peng and M. Xiao, *Nano Lett.*, **3**, 819 (2003).
2. L. Ionov, S. Sapra, A. Synytska, A. L. Rogach, M. Stamm and S. Diez, *Adv. Mater.*, **18**, 1453 (2006).
3. T. A. Taton, C. A. Mirkin and R. L. Letsinger, *Science*, **289**, 1757 (2000).
4. I. Tokareva, S. Minko, J. H. Fendler and E. Hutter, *J. Am. Chem. Soc.*, **126**, 15950 (2004).
5. C. D. Jones and L. A. Lyon, *J. Am. Chem. Soc.*, **125**, 460 (2003).
6. W. Zhang, X. Lei, Z. Wang, D. Zheng, W. Tam, C. Chan and P. Sheng, *Phys. Rev. Lett.*, **84**, 2853 (2000).
7. C. Graf and A. van Blaaderen, *Langmuir*, **18**, 524 (2002).
8. Z. Liang, A. S. Susha and F. Caruso, *Adv. Mater.*, **14**, 1160 (2002).
9. Y. C. Cao, R. Jin and C. A. Mirkin, *Science*, **297**, 1536 (2002).
10. S. Nie and S. R. Emory, *Science*, **275**, 1102 (1997).
11. H. Ko, S. Singamaneni and V. V. Tsukruk, *Small*, **4**, 1576 (2008).
12. C. H. Ho, J. Tobis, C. Sprich, R. Thomann and J. C. Tiller, *Adv. Mater.*, **16**, 957 (2004).
13. M.-C. Daniel and D. Astruc, *Chem. Rev.*, **104**, 293 (2004).
14. M. Grouchko, A. Kamyshny, C. F. Mihailescu, D. F. Anghel and S. Magdassi, *ACS Nano*, **5**, 3354 (2011).

15. L. Polavarapu, K. K. Manga, H. D. Cao, K. P. Loh and Q.-H. Xu, *Chem. Mater.*, **23**, 3273 (2011).
16. A. Kumar, P. K. Vemula, P. M. Ajayan and G. John, *Nat. Mater.*, **7**, 236 (2008).
17. I. Sondi and B. Salopek-Sondi, *J. Colloid Interface Sci.*, **275**, 177 (2004).
18. K. N. Stevens, O. Crespo-Biel, E. E. van den Bosch, A. A. Dias, M. L. Knetsch, Y. B. Aldenhoff, F. H. van der Veen, J. G. Maessen, E. E. Stobberingh and L. H. Koole, *Biomaterials*, **30**, 3682 (2009).
19. J. Wu, N. Zhao, X. Zhang and J. Xu, *Cellulose*, **19**, 1239 (2012).
20. L. Xie, M. Chen and L. Wu, *J. Polym. Sci., Part A: Polym. Chem.*, **47**, 4919 (2009).
21. S. R. Khan, Z. H. Farooqi, M. Ajmal, M. Siddiq and A. Khan, *J. Disp. Sci. Technol.*, **34**, 1324 (2013).
22. A. N. Shipway, E. Katz and I. Willner, *Chem. Phys. Chem.*, **1**, 18 (2000).
23. C. Burda, X. Chen, R. Narayanan and M. A. El-Sayed, *Chem. Rev.*, **105**, 1025 (2005).
24. Z.-J. Jiang, C.-Y. Liu and L.-W. Sun, *J. Phys. Chem. B*, **109**, 1730 (2005).
25. A. C. Patel, S. Li, C. Wang, W. Zhang and Y. Wei, *Chem. Mater.*, **19**, 1231 (2007).
26. H. Sharghi, R. Khalifeh and M. M. Doroodmand, *Adv. Synth. Catal.*, **351**, 207 (2009).
27. F. Alonso, Y. Moglie, G. Radivoy and M. Yus, *Tetrahedron Lett.*, **50**, 2358 (2009).
28. J. Lee, J. C. Park and H. Song, *Adv. Mater.*, **20**, 1523 (2008).
29. R. Heck and J. Nolley Jr., *J. Org. Chem.*, **37**, 2320 (1972).
30. N. Miyaura and A. Suzuki, *Chem. Rev.*, **95**, 2457 (1995).
31. S. Wu, J. Kaiser, X. Guo, L. Li, Y. Lu and M. Ballauff, *Ind. Eng. Chem. Res.*, **51**, 5608 (2012).
32. P. Zhou, Y. Li, P. Sun, J. Zhou and J. Bao, *Chem. Commun.*, 1418 (2007).
33. L. Chen, J. Hu, Z. Qi, Y. Fang and R. Richards, *Ind. Eng. Chem. Res.*, **50**, 13642 (2011).
34. N. Sahiner, H. Ozay, O. Ozay and N. Aktas, *Appl. Catal. B.*, **101**, 137 (2010).
35. M. Rashid and T. K. Mandal, *Adv. Funct. Mater.*, **18**, 2261 (2008).
36. S. Wu, J. Dzubiella, J. Kaiser, M. Drechsler, X. Guo, M. Ballauff and Y. Lu, *Angew. Chem. Int. Ed.*, **51**, 2229 (2012).
37. G. Sharma, Y. Mei, Y. Lu, M. Ballauff, T. Irrgang, S. Proch and R. Kempe, *J. Catal.*, **246**, 10 (2007).
38. S. K. Ghosh, S. Kundu, M. Mandal and T. Pal, *Langmuir*, **18**, 8756 (2002).
39. P. Hervés, M. Pérez-Lorenzo, L. M. Liz-Marzán, J. Dzubiella, Y. Lu and M. Ballauff, *Chem. Soc. Rev.*, **41**, 5577 (2012).
40. C.-H. Tu, A.-Q. Wang, M.-Y. Zheng, X.-D. Wang and T. Zhang, *Appl. Catal. A*, **297**, 40 (2006).
41. A. Biffis, S. Cunial, P. Spontoni and L. Prati, *J. Catal.*, **251**, 1 (2007).
42. A. Biffis and E. Sperotto, *Langmuir*, **19**, 9548 (2003).
43. Y. Mei, Y. Lu, F. Polzer, M. Ballauff and M. Drechsler, *Chem. Mater.*, **19**, 1062 (2007).
44. J. N. Reek, S. Arevalo, R. van Heerbeek, P. C. Kamer and P. W. Van Leeuwen, *Adv. Catal.*, **49**, 71 (2006).
45. X. Gao and I. E. Wachs, *Catal. Today*, **51**, 233 (1999).
46. T. Miyadera, *Appl. Catal. B*, **2**, 199 (1993).
47. M. Valden, X. Lai and D. W. Goodman, *Science*, **281**, 1647 (1998).
48. A. Pich, A. Karak, Y. Lu, A. K. Ghosh and H.-J. P. Adler, *Macromol. Rapid Commun.*, **27**, 344 (2006).
49. H. Naeem, Z. H. Farooqi, L. A. Shah and M. Siddiq, *J. Polym. Res.*, **19**, 1 (2012).
50. Y. Dong, Y. Ma, T. Zhai, F. Shen, Y. Zeng, H. Fu and J. Yao, *Macromol. Rapid Commun.*, **28**, 2339 (2007).
51. D. Suzuki and H. Kawaguchi, *Langmuir*, **22**, 3818 (2006).
52. S. Bhattacharya, F. Eckert, V. Boyko and A. Pich, *Small*, **3**, 650 (2007).
53. Y.-Y. Liu, X.-Y. Liu, J.-M. Yang, D.-L. Lin, X. Chen and L.-S. Zha, *Colloids Surf., A*, **393**, 105 (2012).
54. A. Pich, A. Karak, Y. Lu, A. K. Ghosh and H.-J. P. Adler, *J. Nano. Nanotechnol.*, **6**, 3763 (2006).
55. N. Sahiner, H. Ozay, O. Ozay and N. Aktas, *Appl. Catal. A*, **385**, 201 (2010).
56. S. Carregal-Romero, N. J. Buurma, J. Pérez-Juste, L. M. Liz-Marzán and P. Hervés, *Chem. Mater.*, **22**, 3051 (2010).
57. K. Özlem Nazli, C. W. Pester, A. Konradi, A. Böker and P. van Rijn, *Chem. A Eur. J.*, **19**, 5586 (2013).
58. I. Varga, T. Gilányi, R. Meszaros, G. Filipcsei and M. Zrínyi, *J. Phys. Chem. B*, **105**, 9071 (2001).
59. H. Senff and W. Richtering, *J. Chem. Phys.*, **111**, 1705 (1999).
60. B. R. Saunders and B. Vincent, *Adv. Colloid Interface Sci.*, **80**, 1 (1999).
61. G. M. Eichenbaum, P. F. Kiser, A. V. Dobrynin, S. A. Simon and D. Needham, *Macromolecules*, **32**, 4867 (1999).
62. D. Calvet, J. Y. Wong and S. Giasson, *Macromolecules*, **37**, 7762 (2004).
63. S. Q. Wang, Q. L. Liu and A. M. Zhu, *Eur. Polym. J.*, **47**, 1168 (2011).
64. Z. H. Farooqi, A. Khan and M. Siddiq, *Polym. Int.*, **60**, 1481 (2011).
65. A. Burmistrova, M. Richter, C. Uzum and R. v. Klitzing, *Colloid. Polym. Sci.*, **289**, 613 (2011).
66. M. Ajmal, Z. H. Farooqi and M. Siddiq, *Korean J. Chem. Eng.*, **30**, 2030 (2013).
67. L. M. Liz-Marzán, M. Giersig and P. Mulvaney, *Langmuir*, **12**, 4329 (1996).
68. V. Kozlovskaya, E. Kharlampieva, B. P. Khanal, P. Manna, E. R. Zubarev and V. V. Tsukruk, *Chem. Mater.*, **20**, 7474 (2008).
69. S. Shibu Joseph, B. I. Ipe, P. Pramod and K. G. Thomas, *J. Phys. Chem. B*, **110**, 150 (2006).
70. Y. Murali Mohan, K. Lee, T. Premkumar and K. E. Geckeler, *Polymer*, **48**, 158 (2007).
71. J. Heath, *Phys. Rev. B*, **40**, 9982 (1989).
72. S. Wunder, F. Polzer, Y. Lu, Y. Mei and M. Ballauff, *J. Phys. Chem. C*, **114**, 8814 (2010).
73. S. K. Ghosh, M. Mandal, S. Kundu, S. Nath and T. Pal, *Appl. Catal. A*, **268**, 61 (2004).
74. A. Guillermo, J. Cohen Addad, J. Bazile, D. Duracher, A. Elaissari and C. Pichot, *J. Polym. Sci., Part B: Polym. Phys.*, **38**, 889 (2000).
75. J. T. Zhang, G. Wei, T. F. Keller, H. Gallagher, C. Stötzel, F. A. Müller, M. Gottschaldt, U. S. Schubert and K. D. Jandt, *Macromol. Mater. Eng.*, **295**, 1049 (2010).
76. N. C. Antonels and R. Meijboom, *Langmuir*, **29**, 13433 (2013).
77. R. Vadakkekara, M. Chakraborty and P. A. Parikh, *Colloids Surf., A*, **399**, 11 (2012).